JOURNAL OF CHEMICAL & ENGINEERING DATA

ARTICLE

pubs.acs.org/jced

Cu(II), Co(II), and Mn(II) Complexes of Rhodamine C and Rhodamine 640 Perchlorate: Synthesis, Spectroscopic, Thermal, Fluorescence, and Photostability Studies

Moamen S. Refat,[*,†,‡] Hamada M.A. Killa,[§] Asmaa F. Mansour,[∥] Mohamed Y. Ibrahim,[§] and Hammad Fetooh[§]

[†]Department of Chemistry, Faculty of Science, Port Said University, Port Said, Egypt

[‡]Department of Chemistry, Faculty of Science, Taif University, 888 Taif, Kingdom of Saudi Arabia

[§]Department of Chemistry, Faculty of Science, Zagazig University, Zagazig, Egypt

[∥]Department of Physics, Faculty of Science, Zagazig University, Zagazig, Egypt

ABSTRACT: A goal of our work was to design and synthesize novel Mn(II), Co(II), and Cu(II) complexes with rhodamine C (RHC) and rhodamine 640 perchlorate (RHP) to obtain knowledge about the thermal stability of rhodamine itself compared with its complexes. The complexes prepared have the general formulas $[M(L)_2(H_2O)_2]\cdot nH_2O$ and $[Cu(L)_2]\cdot H_2O$, where (M = Mn(II) or Co(II), L = RHC or RHP, n = 2 or 4). The complexes obtained were characterized using elemental analysis, magnetic measurements, molar conductivity, and infrared and electronic spectra as well as thermal measurements. The results suggested that all the RHC and RHP complexes had a 1:2 molar ratio (metal:L). Both RHC and RHP act as a bidentate chelating ligand through the carboxylic groups. The molar conductance measurements proved that the Mn(II), Co(II), and Cu(II) complexes of RHC and RHP are nonelectrolytes. Kinetic thermodynamic parameters such as E^*, ΔH^*, ΔS^*, and ΔG^* were calculated from differential thermogravimetric curves. The fluorescence and photostability studies were checked for both fluorescence dyes and their complexes.

INTRODUCTION

Laser dyes are very versatile.[1] Rhodamine dyes are widely used as fluorescent probes owing to their high absorption coefficient and broad fluorescence in the visible region of the electromagnetic spectrum, high fluorescence quantum yield, and photostability.[2] Fluorescent molecules are essential for basic research in the biological sciences, the development of new drugs, the assurance of food safety and environmental quality, and the clinical diagnosis of disease.[3,4] Many researchers have designed and synthesized a number of derivatives that have been used as rhodamine-labeled oligonucleotides,[5] pro-fluorophores in a biological environment,[6] fluorescent peptides,[7] inducers and inhibitors,[8] and protease substrates.[9]

In environmental analysis, a new simple, selective, and sensitive fluorescence quenching method was developed to determine chromium using rhodamine 6G. The method was based on the oxidation of rhodamine 6G by chromium(VI) in sulfuric acid solution. The method was applied successfully to the determination of chromium in wastewater and cast iron samples.[10] In 1997, Dujols designed and created a compound with selectivity for Cu(II) in water on the basis of the ion's known reactivity toward rhodamine derivatives.[11] A simple and sensitive fluorescence quenching method for the determination of trace nitrite has also been developed. The method was based on the reaction of rhodamine 110 with nitrite in an acidic medium to form a new compound, which has much lower fluorescence.[12] Generally, the research of rhodamine dyes is a very active field. Rhodamine dyes are used in many applications including spectroscopy, medicine, analysis, biophysical probes, and chemical sensors.[13−20]

MATERIALS AND METHODS

The fluorescent dyes used in the present study (rhodamine C (RHC) (Aldrich), rhodamine 640 perchlorate (RHP) (Aldrich)), the selected transition metal chloride salts $CoCl_2\cdot 6H_2O$, $MnCl_2\cdot 4H_2O$, $CuCl_2\cdot H_2O$, and $NiCl_2\cdot 6H_2O$ (Fluka), and all solvents were of pure or spectroscopic grade. The chemical structures of the fluorescent dyes are given in Figure 1.

Cu(II), Co(II), and Mn(II) Complexes of RHC. These complexes were prepared by adding an appropriate amount of metal salt (0.5 mmol; in 10 mL of 99 % methyl alcohol AR) to a solution of RHC (1 mmol; in 20 mL of methyl alcohol AR), with a molar ratio of 1:2. The pH was adjusted to 11.5 using 0.01 M alcoholic NaOH. The resulting solutions were stirred and refluxed on a hot plate at (60 to 70) °C for 30 min. The volume of the obtained solutions was reduced to half by evaporation and the colored complexes left to precipitate.

Cu(II), Co(II), and Mn(II) Complexes of RHP. The RHP complexes were synthesized by adding Cu(II), Co(II), or Mn(II) chloride (0.05 mmol; in 20 mL of 99 % CH_3OH) to a solution of RHP (0.1 mmol; in 5 mL of distilled H_2O + 15 mL 99 % CH_3OH), with a stiochiometric ratio of 1:2. The pH was adjusted to between 7.0 and 9.0 using 1.0 M NH_4OH dissolved in CH_3OH. The resulting solutions were stirred and heated on a hot plate at (60 to 70) °C for 30 min. The volumes of the obtained solutions were reduced to half by evaporation.

Received: June 17, 2010
Accepted: August 5, 2011
Published: August 22, 2011

Micro Analyses Techniques. The carbon, hydrogen, and nitrogen contents were determined using a Perkin-Elmer CHN 2400 elemental analyzer. The copper(II), cobalt(II), and manganese(II) contents were estimated gravimetrically as metal oxides by direct ignition of the mentioned complexes at 1000 °C for 3 h until constant weight.

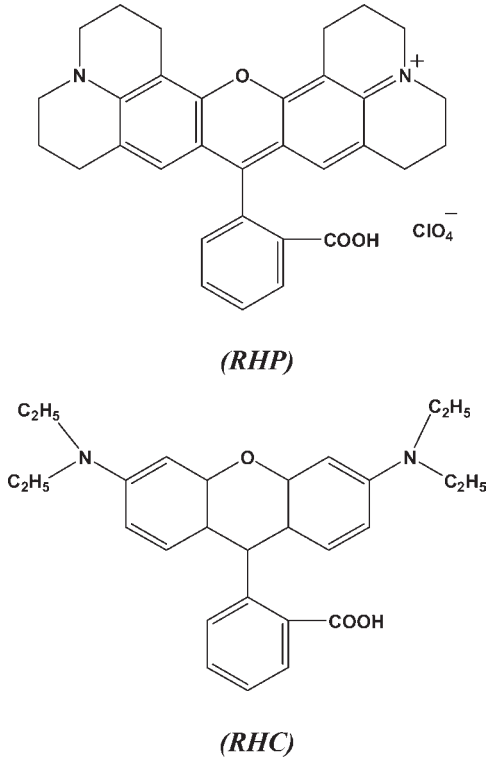

Figure 1. Structures of fluorescent dyes RHP and RHC.

Spectroscopic Investigations. IR spectra were recorded on Bruker FT-IR spectrophotometer [(4000 to 400) cm^{-1}] in KBr disks. The UV−vis spectra were studied in dimethyl sulfoxide (DMSO) solvent at a concentration of $1.0 \cdot 10^{-3}$ M for the fluorescent dyes and their complexes using a Jenway 6405 spectrophotometer with a 1 cm quartz cell in the range (800 to 200) nm. The solid reflectance spectra were performed on a Shimadzu 3101pc spectrophotometer. The purity of the ligands and complexes were checked from their mass spectra at 70 eV by using an AEIMS 30 mass spectrometer with a heating rate of 40 °C/min.

Magnetic Measurements. Magnetic measurements were carried out on a Sherwood Scientific magnetic balance using the Gouy method. Molar conductivities of freshly prepared $1.0 \cdot 10^{-3}$ mol/dm^{-3} DMSO solutions were measured using a Jenway 4010 conductivity meter.

Thermal Investigation. Thermogravimetric analyses (TGA/DTG) were carried out in a nitrogen atmosphere (30 mL/min) with a heating rate of 10 °C/min using a Shimadzu TGA-50H thermal analyzer.

Preparations of Dyed Polymer Matrix. Poly(methyl methacrylate) (PMMA) was purchased from Aldrich. Both PMMA grains and the dye or metal complexes of the dye were dissolved in chloroform and mixed using a magnetic stirrer. The homogeneous mixture was poured into a glass container and allowed to dry.

Optical Absorption. The absorption spectra were recorded using a Perkin-Elmer Lambda 4B spectrophotometer in the range (200 to 900) nm.

Fluorescence Spectra. The fluorescence spectra have been recorded for dyes/PMMA at high concentration ($1 \cdot 10^{-3}$ M) using a Shimadzu RF 5031 PC spectrophotometer.

Dye Photostability. A solar simulator xenon arc lamp "250 w" was used. The degradation of dyes and their complexes was studied by analyzing the UV−vis absorption spectra. The photostability of the dyes was calculated by dividing the absorbance after and before exposure to light. The photostability as a function of exposure time has been obtained.

Table 1. Elemental Analysis and Physical Data of Rhodamine C (RHC) and Its Cu(II), Co(II), and Mn(II) Complexes

			content ((calc) found)				Λ	mp	yield
complexes	color	M_w	% C	% H	% N	% M	(S cm^2 mol^{-1})	(°C)	(%)
$[Mn(RHC)_2(H_2O)_2] \cdot 2H_2O$	reddish	1018.9	(65.95)	(7.46)	(5.50)	(5.39)	87	285	71.3
$(C_{56}H_{76}O_{10}N_4Mn)$	violet		65.22	7.36	5.45	5.27			
$[Co(RHC)_2(H_2O)_2] \cdot 4H_2O$	deep	1058.9	(63.46)	(7.56)	(5.29)	(5.57)	97	> 330	73
$(C_{56}H_{80}O_{12}N_4Co)$	brown		63.32	7.31	5.15	5.33			
$[Cu(RHC)_2] \cdot H_2O$	dark	973.55	(69.03)	(7.19)	(5.75)	(6.53)	83	188	76.9
$(C_{56}H_{70}O_7N_4Cu)$	violet		69.00	6.59	5.64	6.09			

Table 2. Elemental Analyses and Physical Data of Rhodamine 640 Perchlorate (RHP) and Their Cu(II), Co(II), and Mn(II) Complexes

			content ((calc) found)				Λ	mp	yield
complexes	color	M_w	% C	% H	% N	% M	(S cm^2 mol^{-1})	(°C)	(%)
$[Mn(RHP)_2(H_2O)_2] \cdot 2H_2O$	dark red	1307	(58.76)	(5.20)	(4.28)	(4.20)	36	320	82.8
$(C_{64}H_{68}O_{18}N_4Cl_2Mn)$			58.12	5.30	4.07	4.14			
$[Co(RHP)_2(H_2O)_2] \cdot 4H_2O$	bright	1347	(57.02)	(5.35)	(4.16)	(6.38)	47	300	90.3
$(C_{64}H_{72}O_{20}N_4Cl_2Co)$	brown		56.60	5.38	4.15	6.31			
$[Cu(RHP)_2] \cdot H_2O$	bright	1261.5	(60.88)	(4.91)	(4.44)	(5.04)	38	225	88.8
$(C_{64}H_{62}O_{15}N_4Cl_2Cu)$	black		60.56	4.90	4.13	5.01			

dx.doi.org/10.1021/je2007007 |J. Chem. Eng. Data 2011, 56, 3493–3503

Table 3. IR Frequencies (cm^{-1}) of RHC, RHP, and Mn(II)−RHC(I), Co(II)−RHC(II), Cu(II)−RHC(III), Mn(II)−RHP(IV), Co(II)−RHP(V), and Cu(II)−RHP(VI) Complexes

	compounds							
assignments	RHC	RHP	I	II	III	IV	V	VI
ν(OH); H_2O	3412	3423	3447	3449	3445	3422	3446	3423
							3423	
ν_{as}(CH)	3058	3061	2970	2969	2970	3161	2933	2929
	2974	2938	2929	2926	2927	3044		
	2930					2933		
ν_s(CH)	2870	2845	2740	2750	2748	2841	2854	2844
	2712							
ν(COOH)	1704	1719						
ν_{as}(COO^-)	1588	1596	1546	1600	1593	1596	1598	1595
δ_b(H_2O)			1517		1512	1541		
δ(CH)	1467	1496	1445	1440	1459	1493	1458	1456
		1456				1456	1437	1493
						1437	1595	1436
ν_s(COO^-)	1338	1337	1358	1353	1350	1378	1375	1361
		1363				1361		
ν_{as}(CC)	1274	1299	1276	1255	1252	1296	1297	1295
ν(CN)	1246	1199	1253	1282	1221	1183	1186	1184
	1178	1098	1221	1119	1180	1096	1097	1094
	1129	1036	1118	1076	1119	1034	1036	1034
	1074		1077		1076			
ν_s(CC)	974	924	879	914	921	892	893	891
		892		880	879			
δ(CC)	819	775	818		818	771	772	771
	708	725	764		761	729	731	
			700					
ν(M−O)			517	500	542	564	566	567
			463			423	421	423

RESULTS AND DISCUSSION

The results of elemental analysis and some physical properties of the RHC and RHP complexes are discussed. The complexes are air stable with higher melting points, insoluble in H_2O, partially soluble in ethanol and methanol and are soluble in most organic solvents, except for DMSO and dimethylformamide (DMF).

The six isolated solid complexes are $[Mn(RHC)_2(H_2O)_2]\cdot 2H_2O$, $[Co(RHC)_2(H_2O)_2]\cdot 4H_2O$, $[Cu(RHC)_2]\cdot H_2O$, $[Mn(RHP)_2(H_2O)_2]\cdot 2H_2O$, $[Co(RHP)_2(H_2O)_2]\cdot 4H_2O$, and $[Cu(RHP)_2]\cdot H_2O$, which resulted from the interaction between the chloride salts of the Mn(II), Co(II), and Cu(II) ions and the protonated (HL) RHC or RHP ligands. Tables 1 and 2 give the percentage of observed and calculated data of the carbon, hydrogen, nitrogen, and metal(II) ion contents, which are in good agreement with each other and with the predicted structures of the Mn(II), Co(II), and Cu(II) complexes. Accordingly, the mechanism of the complex formation can be summarized in the following equations:

RHC and RHP Complexes

$$MCl_2\cdot xH_2O + 2HL + 2NOH(alc)$$

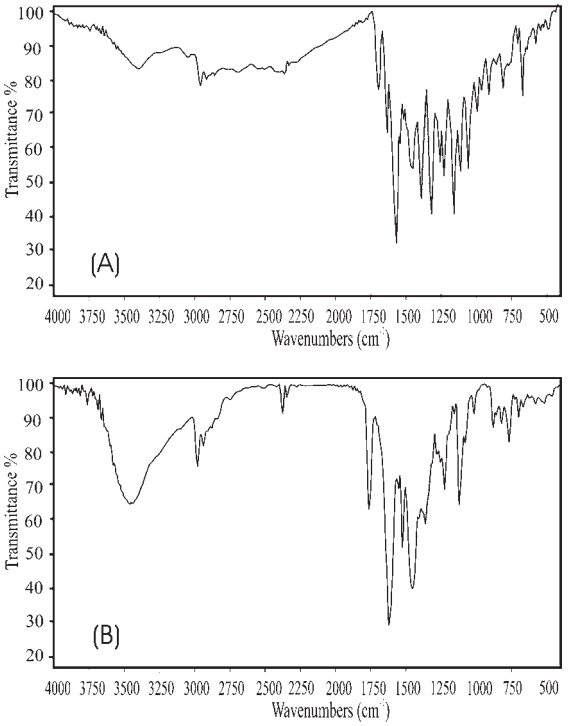

Figure 2. Infrared spectra of (A) RHC and (B) Mn^{2+}−RHC compounds.

$$= [M(L)_2\cdot 2H_2O]\cdot (x-2)H_2O + 2NCl$$

$$+ 2H_2OCuCl_2\cdot H_2O + 2HL + 2NOH(alc)$$

$$= [Cu(L)_2]\cdot H_2O + 2NCl + 2H_2O$$

where M = Mn or Co, L = RHC or RHP, and N = Na (0.01 M with RHC) or NH_4 (1.0 M with RHP).

Molar Conductivities of Metal Chelates. The molar conductivity values of the Mn(II), Co(II), and Cu(II) complexes for both RHC and RHP in DMSO solvent ($1.0\cdot 10^{-3}$ M) are located within the range (36 to 97) Ω^{-1} cm^{-1} M^{-1} and have a nonelectrolyte nature in comparison with the two rhodamine dyes (Tables 1 and 2). The conductivity measurements play an important role in detecting the place of the counterions inside or outside the coordination sphere.[21] According to the molar conductance values, Cl^- anions are absent inside the coordination sphere. These data were matched with the calculated elemental analysis which indicated that Cl^- ions were not detected.

Infrared Spectra. The main infrared bands are summarized in Table 3 and Figures 2 and 3. RHC and RHP exhibited very strong absorption bands at (1704 and 1719) cm^{-1}, respectively, due to the stretching vibration of ν(C═O) for the free ketone of the carboxylic group. This group disappeared in the spectra of their Mn(II), Co(II), and Cu(II) complexes. Two bands appeared at the range (1512 to 1600) cm^{-1} that correspond to $\nu_{as}(COO^-)$, and another band was exhibited within the range (1350 to 1378) cm^{-1} also assigned to $\nu_s(COO^-)$. On the basis of the antisymmetric and symmetric stretching vibration modes ($\nu_{as}(COO^-)$ and $\nu_s(COO^-)$) of the COO^- group, the structure of RHC and RHP complexes can be elucidated.[22] The shift in the values for the frequencies of the $\nu_{as}(COO^-)$ and $\nu_s(COO^-)$

dx.doi.org/10.1021/je2007007 |J. Chem. Eng. Data 2011, 56, 3493–3503

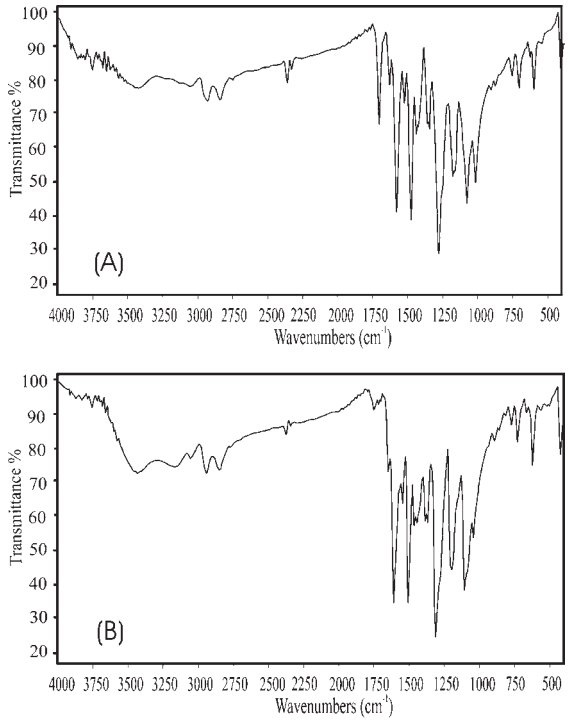

Figure 3. Infrared spectra of (A) RHP and (B) Mn^{2+}−RHP compounds.

bands concerning the free carboxylate ion depends on the coordination mode of the COO^- group with the metal ion. Nakamoto[23] has established that if the coordination is monodentate, the $\nu_{as}(COO^-)$ and $\nu_s(COO^-)$ will be shifted to higher and lower frequencies, respectively. Whereas, if the coordination is chelating bidentate or bridging bidentate, both the $\nu_{as}(COO^-)$ and $\nu_s(COO^-)$ frequencies change in the same direction because the bond orders of both C═O bonds would change by the same amount. On the basis of these facts and comparison of the $\nu_{as}(COO^-)$ and $\nu_s(COO^-)$ frequencies of the RHC and RHP complexes by the $\nu_{as}(COO^-)$ and $\nu_s(COO^-)$ frequencies of sodium carboxylate,[24] as shown in Table 4, it can be said that all the prepared complexes have chelating bidentate structures. The stretching broad band vibration of the OH^- group ν(O−H) occurs as expected[25] around 3400 cm^{-1}. The angular deformation motion of the coordinated water in the hydrated RHC and RHP complexes can be classified into four types of vibrations: δ_b(bend), δ_r(rock), δ_t(twist), and δ_w(wag). The assignments of these motions in all the complexes are as follows: The bending motion, $\delta_b(H_2O)$, is assigned to its characteristic band around 1600 cm^{-1} (from medium to very strong band). The rocking motion, $\delta_r(H_2O)$, is assigned at ∼760 cm^{-1} and the wagging motion, $\delta_w(H_2O)$, is observed at ∼600 cm^{-1}. The twisting motion, $\delta_t(H_2O)$, is observed above 600 cm^{-1}. It should be mentioned here that these assignments for both the bond stretches and angular deformation of the coordinated water molecules fall in the frequency regions reported for related complexes.[23]

Electronic Spectra and Magnetic Measurements. The magnetic moment of the manganese(II) complexes is exhibited at (4.80 and 4.93) BM at room temperature (Table 5), revealing the high spin nature[26] of the complexes having five unpaired electrons. The manganese(II) complexes show bands at around (14 925 to 15 151, 16 949 to 17 241, and 18 518 to 19 047) cm^{-1} assigned to $^5B_{1g} \rightarrow {}^5A_{1g}$, $^5B_{1g} \rightarrow {}^5B_{2g}$, and $^5B_{1g} \rightarrow {}^5E_g$ transitions, respectively, suggesting spin−free manganese(III) complexes with octahedral geometry. The electronic spectra of the Co(II) complexes with RHC and RHP give three bands at about (13 245, 16 666, and 22 222) cm^{-1}. The bands observed are assigned to the transitions, $^4T_{1g}(F) \rightarrow {}^4T_{2g}(F)$ (ν_1), $^4T_{1g}(F) \rightarrow {}^4A_{2g}(F)$ (ν_2), and $^4T_{1g}(F) \rightarrow {}^4T_{2g}(P)$ (ν_3), respectively, suggesting that there is an octahedral geometry around the Co(II) ion.[27−29] The magnetic susceptibility measurements lie in the (5.50 and 5.92) BM range (the normal range for octahedral Co(II) complexes is (4.3 to 5.2) μ_B), which is indicative of octahedral geometry.[30] The electronic spectra of the copper(II) complexes exhibit bands at about (13 513, 20 000, and 25 641) cm^{-1}, which can be assigned to the following three transitions: $^2B_{1g} \rightarrow {}^2B_{2g}$, $^2B_{1g} \rightarrow {}^2A_{1g}$, and $^2B_g \rightarrow {}^2E_g$.[31] These transitions, as well as the measured value of the magnetic moment detected at about 1.85 μ_B is due to a square planar geometry[32] of the copper(II) complexes of RHC and RHP with a coordination number of 4.

The spectra of free RHC and RHP ligands and their Mn(II), Co(II), and Cu(II) complexes in DMSO were scanned. The electronic spectra of the RHC and RHP ligands show absorption bands of aromatic rings and carboxylic groups due to $\pi-\pi^*$ and $n-\pi^*$ intraligand transitions, respectively. These transitions are also found in the spectra of the complexes, but they are shifted toward lower and higher frequencies, confirming the coordination of the ligand with the metallic ions.[32]

Thermal Analysis. Thermal analysis curves (TG/DTG) of the RHC, RHP, and their Mn(II), Co(II), and Cu(II) transition metal complexes were studied and interpreted and the results are given in Tables 6 and 7. For example, the RHC complexes are shown in Figure 4.

RHC and Its Mn(II), Co(II), and Cu(II) Complexes. The RHC ligand decomposed in three stages over the temperature range (30 to 800) °C. The first step occurs at 238 °C in the temperature range [(30 to 280) °C] with a mass loss of 10.31 % (calc = 10.05 %),

Table 4. Asymmetric and Symmetric Stretching Vibrations (cm^{-1}) of the Carboxylate Group

complexes	$\nu_{as}(COO^-)$	$\nu_s(COO^-)$	$\Delta\nu = \nu_{as}(COO^-) - \nu_s(COO^-)$	bonding mode
Mn(II)−RHC	1546	1358	188	bidentate
Co(II)−RHC	1600	1353	247	bidentate
Cu(II)−RHC	1593	1350	243	bidentate
Mn(II)−RHP	1596	1361	235	bidentate
Co(II)−RHP	1598	1375	223	bidentate
Cu(II)−RHP	1595	1361	234	bidentate

Table 5. Magnetic Moment of the Mn(II), Co(II), and Cu(II) Complexes

complexes	μ_{eff} (BM) (found)	μ_{eff} (BM) (calc)	hybrid orbitals	stereochemistry
Mn(II)−RHC	4.80	5.92	sp^3d^2	octahedral
Co(II)−RHC	5.50	5.15	sp^3d^2	octahedral
Cu(II)−RHC	1.85	1.73	dsp^2	square planar
Mn(II)−RHP	4.93	5.92	sp^3d^2	octahedral
Co(II)−RHP	5.92	5.15	sp^3d^2	octahedral
Cu(II)−RHP	1.87	1.73	dsp^2	square planar

dx.doi.org/10.1021/je2007007 |J. Chem. Eng. Data 2011, 56, 3493–3503

Table 6. Thermal Data of the RHC and Its Mn(II), Co(II), and Cu(II) Complexes

				TGA		
		temp range	DTG peak	weight loss (%)		
compounds	steps	(°C)	(°C)	calc	found	assignments
RHC	1	30−280	238	10.05	10.31	COOH
	2	280−400	334	25.89	25.58	$4C_2H_5$
	3	400−800	523	64.06	64.11	−RHC moiety
Mn(II)	1	30−100	48	1.77	1.62	H_2O
	2	100−300	293	8.14	9.58	$3H_2O + C_2H_5$
	3	300−575	628	19.92	20.48	$7C_2H_5$
	4	575−650	779	8.64	8.52	2COO
	5	650−800				MnO_2 residual
Co(II)	1	30−60	42	1.70	2.00	H_2O
	2	60−120	92	3.40	3.62	$2H_2O$
	3	120−200	137	5.10	4.58	$3H_2O$
	4	200−400	478	10.95	10.58	$4C_2H_5$
	5	400−800		19.26	18.95	$4C_2H_5$ + 2COO
						CoO residual
Cu(II)	1	30−170	54	4.82	5.00	$H_2O + C_2H_5$
	2	170−280	258	5.95	6.00	$2C_2H_5$
	3	280−500	426	14.89	14.85	$5C_2H_5$
	4	500−575	515	4.52	4.27	COO
	5	575−800	647, 768	18.75	19.00	COO + remain RHC moiety
						CuO residual

Table 7. Thermal Data of the RHP and Its Mn(II), Co(II), and Cu(II) Complexes

				TGA		
		temp range	DTG peak	weight loss (%)		
compounds	steps	(°C)	(°C)	calc	found	assignments
RHP	1	30−200	46	0	0	solid−solid interaction
	2	200−250	204, 311	14.21	13.31	$6CH_2$
	3	250−300	353	18.95	18.01	$6CH_2+N_2$
	4	300−800	616	66.84	68.68	remain RHP moiety
Mn(II)	1	30−180	51	4.13	3.92	$3H_2O$
	2	180−350	327	14.23	14.45	$12CH_2 + H_2O$
	3	350−500	462	23.87	23.27	$N_2 + 12CH_2$ + 2COO
	4	500−800	535	45.40	45.42	remain RHP moiety
						MnO_2 residual
Co(II)	1	30−150	51	5.34	5.09	$4H_2O$
	2	150−350	300	15.14	15.06	$2H_2O + 12CH_2$
	3	350−450	447	21.08	21.27	$12CH_2+ N_2$ + 2COO
	4	450−800	514	45.55	45.69	COO + remain RHP moiety
						CoO residual
Cu(II)	1	30−350	286	21.71	21.32	H_2O + 2COO + $12CH_2$
	2	350−800	543	66.97	67.21	$12CH_2 + N_2$ + remain RHP moiety
						CuO residual

which is assigned to the loss of the COOH group. The second step starts at 280 °C and ends at 400 °C with a mass loss of 25.58 % (calc = 25.89 %) concerning the loss of four terminal ethyl groups. The last step within the range (400 to 800) °C is accompanied by a mass loss of 64.11 % (calc = 64.06 %). From the corresponding DTG curve, three endothermic peaks are noted. The first maximum is at 238 °C; the second and third are at 334 and 523 °C, respectively.

The thermal decomposition of the Mn(II)−RHC complex occurs in five steps. The first degradation step takes place in the

dx.doi.org/10.1021/je2007007 |J. Chem. Eng. Data 2011, 56, 3493–3503

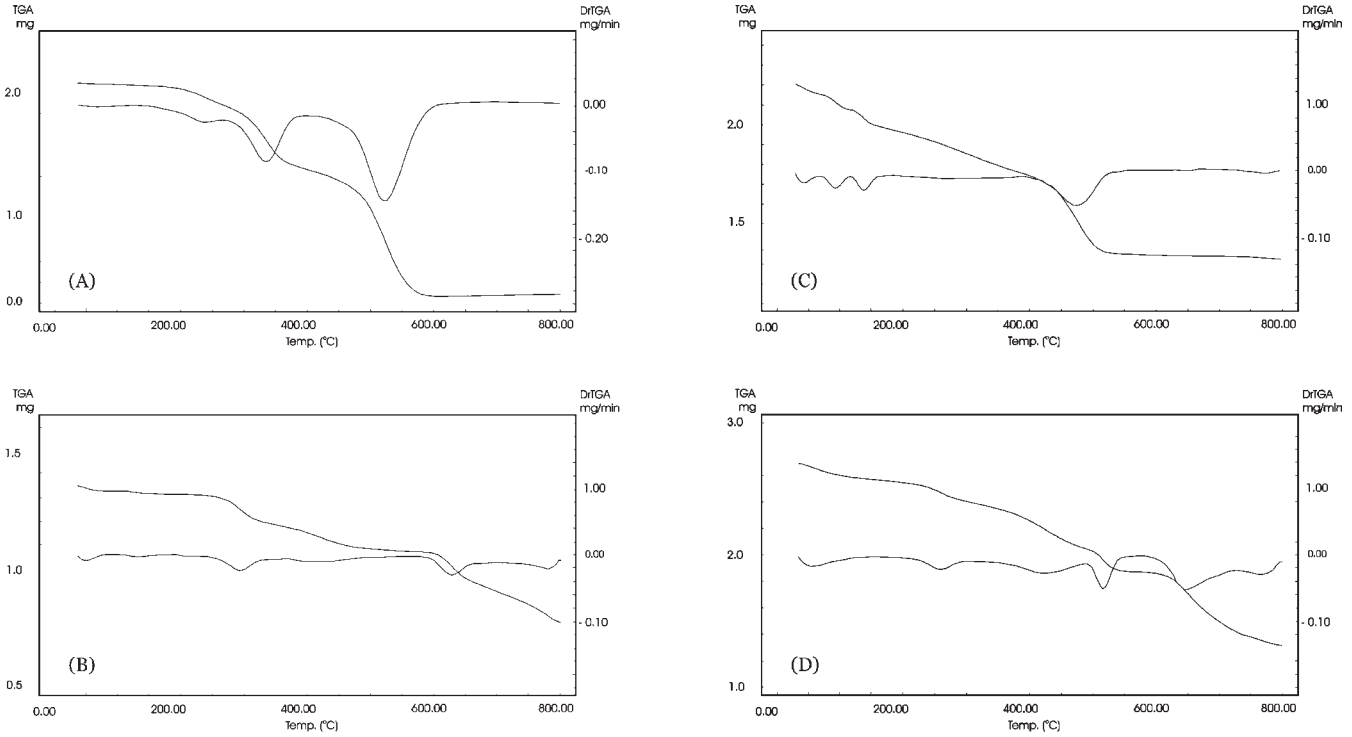

Figure 4. TGA/DTG curves of (A) RHC, (B) Mn^{2+}−RHC, (C) Co^{2+}−RHC, and (D) Cu^{2+}−RHC compounds.

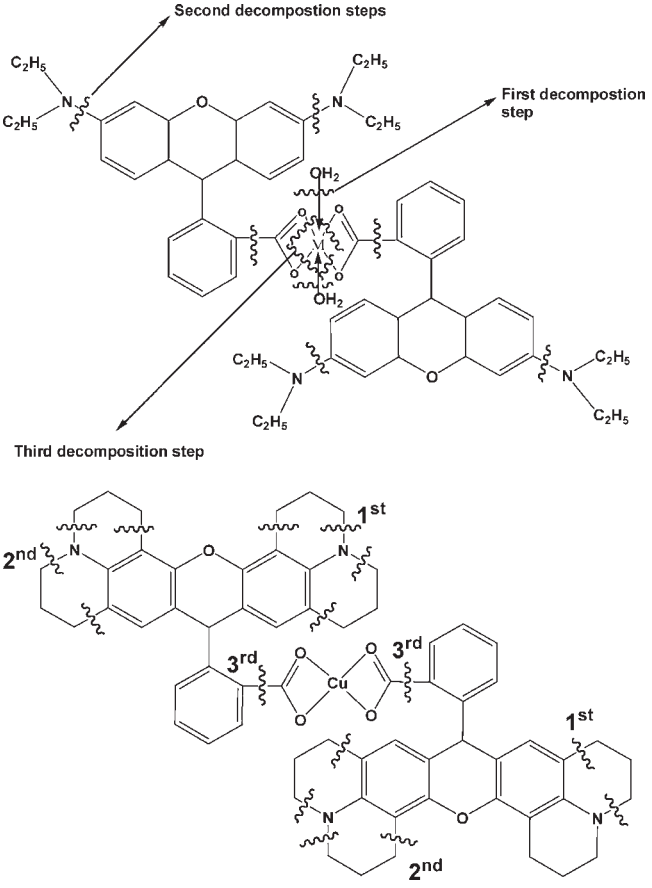

Figure 5. Steps of thermal decompositions of RHP, RHC, and their complexes, where M = Mn(II) and Co(II).

range (30 to 100) °C and corresponds to the elimination of a H_2O molecule with a weight loss of 1.62 % (calc = 1.77 %). The second step falls in the range (100 to 300) °C and is assigned to loss of $3H_2O + C_2H_5$ with a weight loss of 9.58 % (calc =8.14 %). The third and fourth decomposition steps occur within the temperature range (300 to 650) °C and are accompanied by a mass loss of 20.48 % (calc = 19.92 %) and assigned to loss of $7C_2H_5$. The last step occurs within the range (650 to 800) °C with a mass loss of 8.52 % (calc = 8.64 %) due to loss of two COO carboxylate molecules. The MnO_2 is the final product and remains stable until 800 °C.

The thermal decomposition of the Co(II)−RHC complex occurs completely in five steps also. The first step occurs at (30 to 60) °C corresponding to the loss of a H_2O molecule, representing a weight loss of 2.00 % (calc = 1.70 %). The second and third steps occur at (60 to 120) °C and (120 to 200) °C corresponding to the loss of five water molecules, representing a weight loss of 8.20 % (calc = 8.50 %). The fourth and fifth steps are observed at (200 to 400) °C and (400 to 800) °C due to the loss of eight terminal ethyl groups and two carboxylate molecules, with a weight loss of 29.53 % (calc = 30.21 %). CoO is the final product that remains stable until 800 °C.

The Cu(II)−RHC complex decomposes in five steps. The first step occurs at (30 to 170) °C corresponding to the loss of $H_2O + C_2H_5$ molecules representing a weight loss of 5.00 % (calc = 4.82 %). The second and third steps occur at (170 to 500) °C and correspond to the loss of seven C_2H_5 organic molecules. The weight loss associated with these steps is 20.85 % (calc = 20.84 %). The fourth and fifth steps exist within the range (500 to 800) °C and are assigned to the loss of two carboxylate groups and RHC molecule. The mass loss due to these steps is 23.27 % (calc = 23.27 %). The final residue at the end of this stage is CuO.

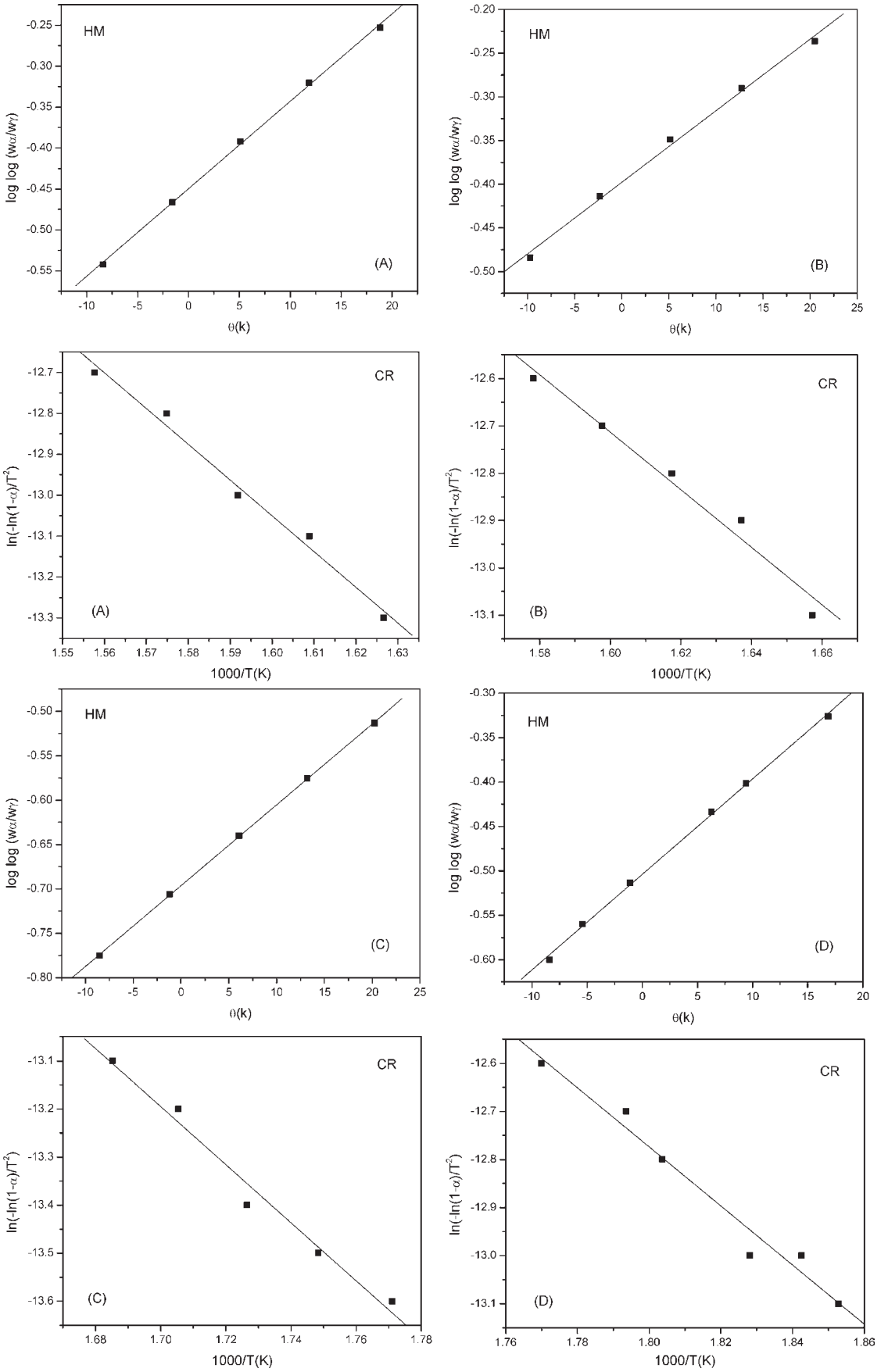

Figure 6. Kinetic data of (A) RHP, (B) Mn^{2+}−RHP, (C) Co^{2+}−RHP, and (D) Cu^{2+}−RHP compounds.

dx.doi.org/10.1021/je2007007 |J. Chem. Eng. Data 2011, 56, 3493–3503

Table 8. Kinetic Parameters Using the Coats−Redfern (CR) and Horowitz−Metzger (HM) Equations for the RHC and Its Mn(II), Co(II), and Cu(II) Complexes

			parameter					
			E	A	ΔS	ΔH	ΔG	
complex	stage	method	(J mol^{-1})	(s^{-1})	(J mol^{-1} K^{-1})	(J mol^{-1})	(J mol$^{-1)}$	r
RHC	2nd	CR	$1.06 \cdot 10^5$	$5.01 \cdot 10^{12}$	$-7.07 \cdot 10^1$	$1.55 \cdot 10^5$	$1.59 \cdot 10^5$	0.9973
		HM	$1.07 \cdot 10^5$	$9.14 \cdot 10^{13}$	$-1.71 \cdot 10^1$	$1.65 \cdot 10^5$	$1.56 \cdot 10^5$	0.9974
		average	$1.06 \cdot 10^5$	$4.28 \cdot 10^{13}$	$-4.39 \cdot 10^1$	$1.60 \cdot 10^5$	$1.57 \cdot 10^5$	
Mn(II)	2nd	CR	$1.11 \cdot 10^5$	$2.74 \cdot 10^7$	$-1.09 \cdot 10^2$	$1.06 \cdot 10^5$	$1.73 \cdot 10^5$	0.9942
		HM	$1.15 \cdot 10^5$	$5.23 \cdot 10^7$	$-1.03 \cdot 10^2$	$1.09 \cdot 10^5$	$1.73 \cdot 10^5$	0.9994
		average	$1.13 \cdot 10^5$	$3.98 \cdot 10^7$	$-1.06 \cdot 10^2$	$1.07 \cdot 10^5$	$1.73 \cdot 10^5$	
Co(II)	1st	CR	$5.32 \cdot 10^4$	$1.38 \cdot 10^6$	$-1.28 \cdot 10^2$	$5.05 \cdot 10^4$	$9.12 \cdot 10^4$	0.9794
		HM	$5.67 \cdot 10^4$	$3.42 \cdot 10^7$	$-1.01 \cdot 10^2$	$5.04 \cdot 10^4$	$8.63 \cdot 10^4$	0.9857
		average	$5.49 \cdot 10^4$	$3.55 \cdot 10^6$	$-1.14 \cdot 10^2$	$5.04 \cdot 10^4$	$8.87 \cdot 10^4$	
Cu(II)	1st	CR	$6.21 \cdot 10^4$	$4.68 \cdot 10^9$	$-9.88 \cdot 10^1$	$5.94 \cdot 10^4$	$9.02 \cdot 10^4$	0.9916
		HM	$7.04 \cdot 10^4$	$4.09 \cdot 10^9$	$-6.01 \cdot 10^1$	$6.77 \cdot 10^4$	$8.72 \cdot 10^4$	0.9944
		average	$6.62 \cdot 10^4$	$4.38 \cdot 10^9$	$-7.94 \cdot 10^1$	$6.35 \cdot 10^4$	$8.87 \cdot 10^4$	

Table 9. Kinetic Parameters Using the Coats−Redfern (CR) and Horowitz−Metzger (HM) Equations for the RHP and Its Mn(II), Co(II), and Cu(II) Complexes

			parameter					
			E	A	ΔS	ΔH	ΔG	
complex	stage	method	(J mol^{-1})	(s^{-1})	(J mol^{-1} K^{-1})	(J mol^{-1})	(J mol$^{-1)}$	r
RHP	1st	CR	$5.05 \cdot 10^4$	$7.62 \cdot 10^1$	$-2.15 \cdot 10^2$	$4.54 \cdot 10^4$	$1.77 \cdot 10^5$	0.9870
		HM	$5.09 \cdot 10^4$	$4.97 \cdot 10^2$	$-1.99 \cdot 10^2$	$5.39 \cdot 10^4$	$1.76 \cdot 10^5$	0.9979
		average	$5.07 \cdot 10^4$	$2.86 \cdot 10^2$	$-2.07 \cdot 10^2$	$4.96 \cdot 10^4$	$1.76 \cdot 10^5$	
Mn(II)	2nd	CR	$7.26 \cdot 10^4$	$5.46 \cdot 10^3$	$-1.08 \cdot 10^2$	$6.74 \cdot 10^4$	$1.79 \cdot 10^5$	0.9938
		HM	$7.94 \cdot 10^4$	$2.79 \cdot 10^4$	$-1.66 \cdot 10^2$	$7.42 \cdot 10^4$	$1.78 \cdot 10^5$	0.9995
		average	$7.61 \cdot 10^4$	$1.66 \cdot 10^4$	$-1.37 \cdot 10^2$	$7.08 \cdot 10^4$	$1.78 \cdot 10^5$	
Co(II)	2nd	CR	$5.02 \cdot 10^4$	$8.11 \cdot 10^2$	$-2.14 \cdot 10^2$	$4.55 \cdot 10^4$	$1.68 \cdot 10^5$	0.9895
		HM	$5.72 \cdot 10^4$	$8.63 \cdot 10^2$	$-1.94 \cdot 10^2$	$5.25 \cdot 10^4$	$1.64 \cdot 10^5$	0.9999
		average	$5.37 \cdot 10^4$	$8.37 \cdot 10^2$	$-2.04 \cdot 10^2$	$4.90 \cdot 10^4$	$1.66 \cdot 10^5$	
Cu(II)	1st	CR	$5.11 \cdot 10^4$	$2.76 \cdot 10^2$	$-2.03 \cdot 10^2$	$4.65 \cdot 10^4$	$1.58 \cdot 10^5$	0.9857
		HM	$6.02 \cdot 10^4$	$4.98 \cdot 10^3$	$-1.79 \cdot 10^2$	$5.81 \cdot 10^4$	$1.56 \cdot 10^5$	0.9994
		average	$5.56 \cdot 10^4$	$2.62 \cdot 10^3$	$-1.91 \cdot 10^2$	$5.23 \cdot 10^4$	$1.57 \cdot 10^5$	

RHP and Its Mn(II), Co(II), and Cu(II) Complexes. The thermal decomposition of the free RHP ligand proceeds approximately with five degradation steps. The first stage occurs at a maximum temperature of 46 °C with no weight loss due to solid−solid interaction. The second and third stages occur at maximum temperatures of (204 and 311) °C, respectively, with the weight loss associated with these stages being 13.31 % (calc = 14.21 %) corresponding to the loss of $6CH_2$. The fourth step occurs at a maximum temperature of 353 °C, with a weight loss of 18.01 % (calc = 18.95 %) associated with the loss of $6CH_2 + N_2$. The final decomposition stage occurs at a maximum temperature of 616 °C. The weight loss at this step is 68.68 % (calc = 66.84 %) associated with the loss of remaining RHP molecule.

The thermal degradation of the Mn(II)−RHP complex occurs in mainly four degradation stages. The first stage of decomposition occurs at a temperature maximum of 180 °C. The found weight loss associated with this step is 3.92 % (calc = 4.13 %) and may be attributed to the loss of $3H_2O$. The second step of decomposition occurs at a temperature maximum of 327 °C. The weight loss found at this step equals 14.45 % (calc = 14.23 %) corresponding to the loss of $12CH_2 + H_2O$. The third step of decomposition occurs at a temperature maximum of 500 °C. The weight loss found associated with this step is 23.27 % (calc = 23.87 %) and may be attributed to the loss of $N_2 + 12CH_2 + 2COO$. The final step occurred at (500 to 800) °C corresponds to the loss of remaining RHP organic moiety. The final thermal product obtained at 800 °C is MnO_2.

The Co(II)−RHP complex also has four decomposition steps. These steps are located in the range between (30 to150) °C, (150 to 350) °C, (350 to 450) °C, and (450 to 800) °C and the weight loss for the first step is 5.09 % (calc = 5.34 %) due to the loss of $4H_2O$. The second decomposition stage occurs at a maximum temperature of 300 °C. The weight loss at this step is 15.06 % (calc = 15.14 %) associated with the loss of $2H_2O + 12CH_2$. The

dx.doi.org/10.1021/je2007007 |J. Chem. Eng. Data 2011, 56, 3493–3503

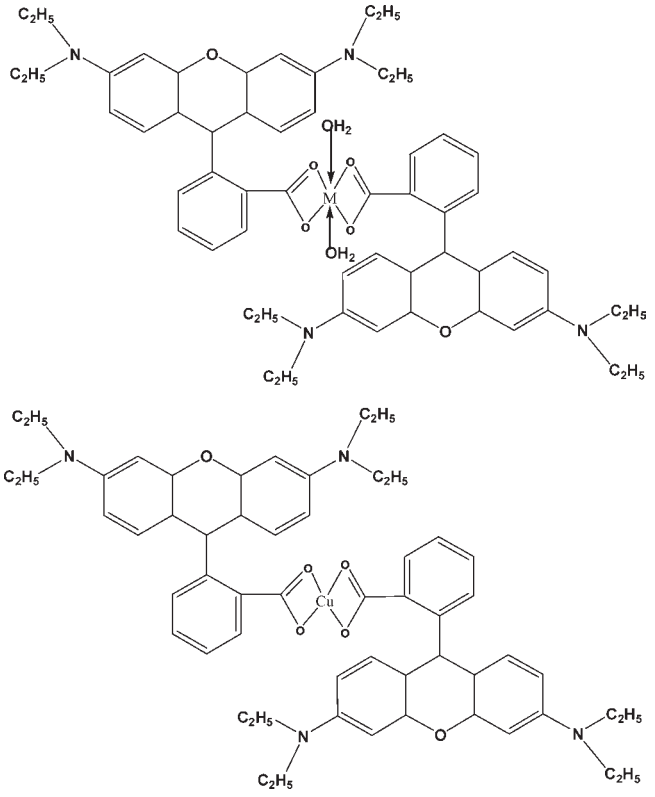

Figure 7. Mode of chelations of the RHC and RHP complexes, where M = Mn(II) and Co(II).

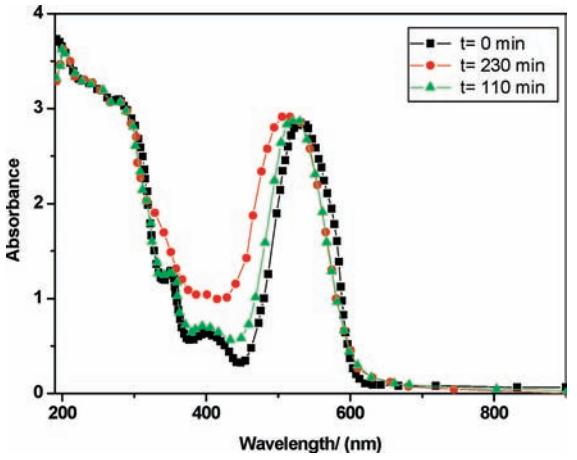

Figure 8. Photostability of rhodamamine C doped in PMMA before and after exposure to UV−vis light.

third step of the degradation occurs at a maximum temperature of 447 °C and is accompanied by a weight loss of 21.27 % (calc = 21.08 %) corresponding to the loss of $12CH_2 + N_2 + 2COO$. The observed weight loss of the final decomposition stage is 45.69 % associated with the loss of remaining RHP organic part. The final residue at the end of this stage is CoO.

The thermal decomposition of the Cu(II)−RHP complex proceeds with two main degradation steps. The first decomposition stage occurs at a maximum temperature of 286 °C. The weight loss at this step is 21.32 % (calc = 21.71 %) associated with the loss of H_2O + 2COO +$12CH_2$. The final decomposition

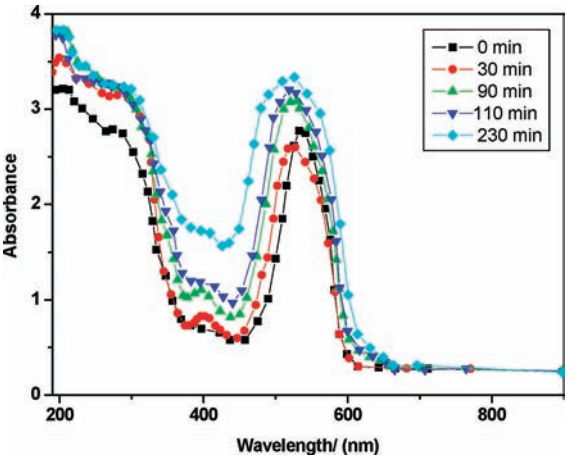

Figure 9. Photostability of the rhodamamine C−Mn^{2+} complex doped in PMMA before and after exposure to UV−vis light.

stage occurs at a maximum temperature of 543 °C. The observed weight loss at this step is 67.21 % associated with the loss of N_2 + $12CH_2$+ remaining RHP moiety. The final residue at the end of this stage is CuO.

From the above discussion concerning the steps of thermal degradation, it is clear that the data resulting from the elemental analysis match the thermal analysis data, which confirms that the molar ratio between the metal and RHC or RHP is 1:2. This is obvious from the liberation of two carboxylate groups and eight ethyl groups. We can conclude the steps of thermal decomposition as shown in Figure 5.

Kinetic Studies. The thermodynamic activation parameters of the decomposition processes of the hydrated Mn(II), Co(II), and Cu(II) complexes, namely activation energy (E^*), enthalpy (ΔH^*), entropy (ΔS^*), and Gibbs energy of the decomposition (ΔG^*), were evaluated graphically (Figure 6) by employing the Coats−Redfern and Horowitz−Metzger relations.[33,34]

$$\Delta H^* = E^* - RT$$

$$\Delta G^* = \Delta H^* - T\Delta S^*$$

The data obtained are summarized in Tables 8 and 9. The activation energies of decomposition are in the range (113 to 761) kJ mol^{-1}. The high values of the activation energy reflect the thermal stability of the complexes. The entropy of activation is negative for all complexes, which indicates that RHC and RHP complexes are more ordered than the reactants.

Chelating Mode of the RHC and RHP Complexes. The structures of the complexes of RHC and RHP with the Mn(II), Co(II), and Cu(II) ions were confirmed using elemental analyses, IR, molar conductance, magnetic, solid reflectance, UV−vis, and thermal analysis data. Therefore, from the IR spectra, it is concluded that both RHC and RHP behave as bidentate ligands, coordinated to the metal ions via the carboxylate group. RHC and RHP behave as uninegative bidentate ligands, coordinated to the metal ions via a deprotonated COOH group. From the molar conductance data, it was found that the RHC and RHP complexes are considered 1:2 nonelectrolytes. On the basis of the above observations and from the magnetic and solid reflectance measurements, octahedral and square planar geometries are suggested for the investigated complexes.

dx.doi.org/10.1021/je2007007 |J. Chem. Eng. Data 2011, 56, 3493–3503

Table 10. Rate Constants (k) of Photodegradation and Half-Life Times of Doped Dyes and Their Metal Complexes in PMMA

sample	k (min^{-1})		$t_{1/2}$ (min)	
rhodamamine C/PMMA	513 nm	200 nm	513 nm	200 nm
	$1.374 \cdot 10^{-4}$	$2.452 \cdot 10^{-4}$	5044	2827
rhodamamine C/Mn^{2+} complex/PMMA	522 nm	200 nm	522 nm	200 nm
	$6.775 \cdot 10^{-4}$	$5.3 \cdot 10^{-4}$	1023	1308

Table 11. Spectroscopic Parameters of Rhodamamine C and Rhodamamine C−Mn^{2+} Complex of Concentration $1 \cdot 10^{-3}$ M Doped in PMMA before and after Irradiation to UV−Vis Light

sample	λ_{abs} (nm)	λ_{em} (nm)	$\Delta\lambda_s$ (nm)	φ_F (%)
rhodamamine C before irradiation	529	569	40	81.1
rhodamamine C after irradiation	513	569	56	46.2
rhodamamine C/Mn^{2+} complex before irradiation	537	569	32	71.9
rhodamamine C/Mn^{2+} complex after irradiation	522	569	47	41.9

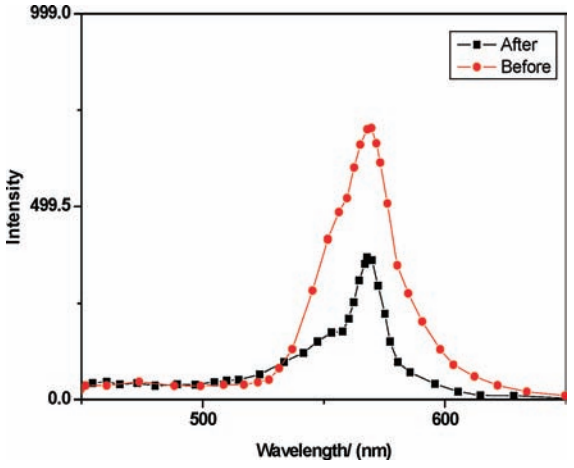

Figure 10. Fluorescence spectrum of rhodamamine C before and after irradiation to UV−vis light.

As a general conclusion, the investigated metal complex structures can be given (Figure 7).

Photostability of Fluorescence Dyes and Their Metal Complexes. In case of rhodamine C undoped, highly delocalized bonds (C═C and C═O) are mainly affected by UV−vis radiation (photodegradation). Also the photochemical degradation of rhodamine C doped in PMMA occurs only in the presence of suitable optical radiation, which produces large local increases in temperature and thermal destruction of the dye molecules.[35] At the xenon arc lamp power used, there is no general consensus concerning the mechanism responsible for thermal damage of polymeric materials. It can be seen that the dye molecules embedded in the PMMA matrix do not undergo any changes in chemical properties at low power.[35] Rhodamine C doped in PMMA was exposed indoors to UV−vis radiation, and

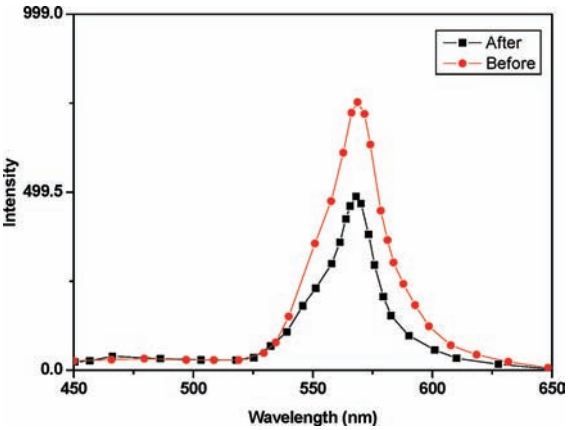

Figure 11. Fluorescence spectrum of rhodamamine C−Mn^{2+} complex before and after irradiation to UV−vis light.

the change in the absorption spectra was achieved at different times during the irradiation period (230 and 480 min, respectively), as shown in Figure 8. Also, the rhodamamine C−Mn^{2+} complex doped in PMMA showed after exposure to UV−vis radiation an enhancement of the photostability, as presented in Figure 9. The increase in photostability is due to strong chelation (complexation of dye with metal). The rate constant of the photodegradation of the dyes was estimated according to the following equation.[36]

$$k = \frac{2.303}{t} \log \frac{A_0}{A}$$

where A_0 and A are the absorption before and after irradiation for time (t). The k value and half-life times are listed in Table 10. It is clear from the degradation data that the complexation modifies the photostability of the dye.[37]

Fluorescence Spectroscopy of Samples. The fluorescence spectra of the samples give a very low intensity except for rhodamine C and the rhodamine C−Mn^{2+} complex, which show good fluorescence intensity. The fluorescence quantum yields of rhodamine C and the rhodamine C−Mn^{2+} complex have been calculated relative to the rhodamine 6G (Rh 6G) dye as a reference ($\phi_F \approx 90$ %) from the following equation[38] and are listed in Table 11.

$$\phi_F = \phi_{F,ref}(A_{ref}/A)(n/n_{ref})(a/a_{ref})$$

where $\varphi_{F,ref}$ is the fluorescence quantum yield of the reference, A is the absorbance at the excitation wavelength, n is the index of refraction and a is the area under the fluorescence curve. From Table 11 some notes can be detected:

1. The value of the fluorescence quantum yield for rhodamine C is decreased by irradiation for 230 min by 43 %, and the value of φ_F for the rhodamine C−Mn^{2+} complex after

dx.doi.org/10.1021/je2007007 |J. Chem. Eng. Data 2011, 56, 3493–3503

irradiation for 230 min is decreased by 41.7 %. The fluorescence spectra are shown in Figures 10 and 11, respectively.
2. The wavelength of the maximum absorption is blue-shifted after irradiation.
3. The values of the Stokes shift $\Delta\lambda_s$ are increased by irradiation, which indicates that the overlap between the absorption and fluorescence spectra decreased, so the fluorescence is not reabsorbed by another dye molecule of the same type, which is termed self-absorption and is actually a dominant effect over the long path lengths traveled by light trapped in the forward scatter (FSC).

AUTHOR INFORMATION

Corresponding Author

*E-mail: msrefat@yahoo.com.

REFERENCES

(1) Duarte, F. J. *High Power Dye Lasers*; Springer-Verlag: Berlin, 1991.

(2) Beija, M.; Afonso, C. A. M.; Martinho, J. M. G. Synthesis and applications of rhodamine derivatives as fluorescent probes. *Chem. Soc. Rev.* **2009**, *38*, 2410–2433.

(3) Valeur, B. Development of Rhodamine Dyes for Biochemical Application. In *Molecular Fluorescence: Principles and Applications [M]*; Zhang, L., et al., Eds.; Wiley-VCH: Weinheim, 2002.

(4) Mason, W. T. *Fluorescent and Luminescent Probes for Biological Activity*, 2nd ed. [M]; Academic Press: San Diego, CA, 1999.

(5) Ravi, V. A convenient, solid-phase coupling of rhodamine dye acids to 5′ amino-oligonucleotides. *Tetrahedron Lett.* **1999**, *40*, 7611–7613.

(6) Chandran, S. S.; Dickson, K. A.; Raines, R. T. Latent fluorophore based on the trimethyl lock. *J. Am. Chem. Soc.* **2005**, *127* (6), 1652–1653.

(7) Houghten, R. A.; Dooley, C. T.; Appel, J. R. De novo identification of highly active fluorescent kappa opioid ligands from a rhodamine labeled tetrapeptide positional scanning library. *Bioorg. Med. Chem. Lett.* **2004**, *14* (8), 1947–1951.

(8) Cai, S. X.; Zhang, H. Z.; Guastella, J.; Drewe, J.; Yang, W.; Weber, E. Design and synthesis of Rhodamine 110 derivative and Caspase-3 substrate for enzyme and cell-based fluorescent assay. *Bioorg. Med. Chem. Lett.* **2001**, *11*, 39–42.

(9) Leytus, S. P.; Melhado, L. L.; Mangel, W. F. Rhodamine-based compounds as fluorogenic substrates for serine proteinases. *Biochem. J.* **1983**, *209* (2), 299–307.

(10) Jie, N.; Zhang, Q.; Yang, J.; Huang, X. Determination of chromium in waste-water and cast iron samples by fluorescence quenching of rhodamine 6G. *Talanta* **1998**, *46* (1), 215–219.

(11) Dujols, V.; Ford, F.; Czarnik, A. W. A long-wavelength fluorescent chemodosimeter selective for Cu(II) ion in water. *J. Am. Chem. Soc.* **1997**, *119*, 7386–7387.

(12) Zhang, G. D.; Harada, A.; Nishiyama, N.; Jiang, D. L.; Koyama, H.; Aida, T.; Kataoka, K. Polyion complex micelles entrapping cationic dendrimer porphyrin: effective photosensitizer for photodynamic therapy of cancer. *J. Controlled Release* **2003**, *93* (2), 141–150.

(13) Zhang, X.; Wang, H.; Fu, N.-N.; Zhang, H.-S. A fluorescence quenching method for the determination of nitrite with Rhodamine 110. *Spectrochim. Acta A* **2003**, *59* (8), 1667–1672.

(14) Demas, J. N.; DeGraff, B. A. Applications of Luminescent Transition Metal Complexes to Sensor Technology and Molecular Probes. *J. Chem. Educ.* **1997**, *74* (6), 690–695.

(15) Demas, J. N.; DeGraff, B. A. Design and Applications of Highly Luminescent Transition Metal Complexes. *Anal. Chem.* **1991**, *63*, 829A–837A.

(16) Demas, J. N.; DeGraff, B. A. In *Topics in Fluorescence Spectroscopy: Probe Design and Chemical Sensing*; Lakowicz, J. R., Ed.; Plenum Press: New York, 1994; Vol. 4, pp 71−107.

(17) Lakowicz, J. R.; Terpetschnig, E.; Murtaza, Z.; Szmacinski, H. Development of Long-Lifetime Metal-Ligand Probes for Biophysics and Cellular Imaging. *J. Fluoresc.* **1997**, *7* (1), 17–25.

(18) Terpetschnig, E.; Szmacinski, H.; Lakowicz, J. R. Long-Lifetime Metal-Ligand Complexes as Probes in Biophysics and Clinical Chemistry. In *Methods in Enzymology*; Academic Press: London, 1997; Vol. 278, pp 295−321.

(19) Shakhverdov, T. A.; Ergashev, R. Amiodarone protects cardiac myocytes against oxidative injury. *Opt. Spektrosk.* **1999**, *87* (2), 236–242.

(20) Qu, J. Q.; Wang, L. F.; Li, Y. Z.; Sun, G. C.; Zhu, Q. J.; Xia, C. G. Synthesis and X-ray crystal structure of a Cd(II) Complex of rhodamine B. *Synth. React. Inorg. Metal-Org. Nano-Met. Chem.* **2001**, *31*, 1577–1585.

(21) Burger, K. *Coordination Chemistry: Experimental Methods*, 1st ed.; Butterworth Group: London, 1973.

(22) Maciejewski, M. Concepts of Trapping Topologically by Shell Molecules. *J. Macromol. Sci. Chem. A* **1982**, *17* (4), 689–703.

(23) Nakamoto, K. *Infrared and Raman Spectra of Inorganic and Coordination Compounds*, 3rd ed.; John Wiely & Sons, Inc.: New York, 1978.

(24) Nakanishi, K.; Solomon, P. H. *Infrared Absorption Spectroscopy*; 2nd ed.; Holden-Day, Inc.: New York, 1977; p 33.

(25) Abd El-Wahed, M. G.; Refat, M. S.; El-Megharbel, S. M. Spectroscopic, thermal and biological studies of the coordination compounds of sulfasalazine drug: Mn(II), Hg(II), Cr(III), ZrO(II), VO(II) and Y(III) transition metal complexes. *Chem. Pharm. Bull.* **2008**, *56* (11), 1585–1591.

(26) Aswar, A. S.; Mandlik, P. R.; Aswale, S. R. Chromium (III), Manganese (III), Iron (III), Oxovanadium (IV), Zirconium (IV) & dioxouranium (II) complexes of hydrazone of isonicotinic acid hydrazide. *J. Indian Chem. Soc.* **2002**, *79*, 689–692.

(27) Mondal, N.; Dey, D. K.; Mitra, S.; Abdul, M. K. M. Synthesis and structural characterization of mixed ligand η1−2-hydroxyacetophenone complexes of cobalt(III). *Polyhedron* **2000**, *19*, 2707–2711.

(28) Kohout, J.; Hvastijova, M.; Kozisek, J.; Diaz, J. G.; Valko, M.; Jager, L.; Svoboda, I. Cyanamidonitrate−copper(II) complexes of imidazole ligands: X-ray crystallography and physical investigation. *Inorg. Chim. Acta* **1999**, *287* (2), 186–192.

(29) Bury, A.; Underhill, A. E.; Kemp, D. R.; O'Shea, N. J.; Smith, J. P.; Gomm, P. S. Hallway, F. Metal complexes of anti-inflammatory drugs. Part IV. Tenoxicam complexes of manganese(II), iron(III), cobalt(II), nickel(II) and copper(II). *Inorg. Chim. Acta* **1987**, *138*, 85–9.

(30) Kumar, N. R. S.; Nethiji, M.; Patil, K. C. Preparation, characterization, spectral and thermal analyses of $(N_2H_5)_2MCl_4 \cdot 2H_2O$ (M = Fe, Co, Ni and Cu); crystal structure of the iron complex. *Polyhedron* **1991**, *10* (3), 365–371.

(31) Konstantinovic, S. S.; Radovanovic, B. C.; Krkljes, A. Thermal behaviour of Co(II), Ni(II), Cu(II), Zn(II), Hg(II) and Pd(II) complexes with isatin-β-thiosemicarbazone. *J. Therm. Anal. Cal* **2007**, *90* (2), 525–531.

(32) Lever, A. B. P. *Inorganic Electronic Spectroscopy*, 4th ed.; Elsevier: London, 1984; p 481.

(33) Coats, A. W.; Redfern, J. P. Kinetic parameters from thermogravimetric data. *Nature* **1964**, *201*, 68–69.

(34) Horowitz, H. W.; Metzger, G. A new analysis of thermogravimetric traces. *Anal. Chem.* **1963**, *35*, 1464–1468.

(35) Kim, O.-K.; Lee, K.-S.; Huang, Z.; Heuer, W. B.; Paik-Sung, C. S. Oligothiophene as photonic/electronic property modulator. *Opt. Mater.* **2002**, *21*, 559–564.

(36) Grabchev, I.; Bojinov, V. Synthesis and Characterisation of Fluorescent Polyacrylonitrile Copolymers with 1,8-Naphthalimide Side Chains. *Polym. Degrad. Stab.* **2000**, *70*, 147–153.

(37) Esumi, K.; Hayakawa, K.; Yoshimura, T. Morphological change of gold-dendrimer nanocomposites by laser irradiation. *J. Colloid Interface Sci.* **2003**, *268* (2), 501–506.

(38) Demas, J. N.; Grosby, G. A. The Measurement of Photoluminescence Quantum Yields. *J. Phys. Chem.* **1971**, *75*, 991–1024.